JOURNAL OF APPLIED ELECTROCHEMISTRY 2 (1972) 289–299

Electrolytic removal of oxygen from gases by means of solid electrolyte

C. B. ALCOCK AND S. ZADOR

Department of Metallurgy and Materials Science, University of Toronto, Canada

Received 3 December 1971 and in revised form 6 April 1972

Nitrogen gas, containing controlled amounts of free oxygen and water or carbon dioxide, was de-oxidized by means of a solid oxide electrolyte tube at temperatures from 800 to 1000°C and at applied voltages of 0·5–3·0 V. The oxygen potential of the resulting gas mixture was measured simultaneously. The efficiency of the removal of oxygen, present in free or combined state, is shown as a function of the initial oxygen content P_{H_2O}, P_{CO_2}, temperature and applied voltage. The electrolysing current/applied voltage relationships obtained indicate that the resistance of the electrolysing circuit is mainly determined by the initial free oxygen content of the gas mixture. The behaviour of solid oxide electrolytes with externally applied potentials corresponding to pure ionic and mixed conduction is also discussed.

1. Introduction

The use of solid oxide electrolytes in measuring the oxygen chemical potential of gases has had many applications [1–3], but relatively little work has been reported on the behaviour of systems incorporating solid electrolytes during electrolysis [4, 5]. In the present study, the extent of the removal of oxygen from a flowing gaseous system was studied for a number of initial oxygen contents, and in the presence of gaseous compounds containing oxygen—i.e., H_2O and CO_2. The relation between the oxygen content of the gaseous phase, either free or combined, and the electrolysing current was investigated as a function of the applied voltage and the analysis of the results shows that the processes taking place in solid electrolytes during the application of an external voltage and the passage of current, are dependent on the magnitudes of these variables.

2. Experimental

2.1. *Apparatus*

A horizontal Kanthal-wound resistance furnace, the temperature of which was controlled by means of a 'Thermo-electric 400' solid state controller, was used to heat an alumina (Purox) reaction tube of approximately 19 mm internal diameter. A brass head, fitted on one end of this tube, held a 12·7 mm i.d. lime-stabilized zirconia tube (manufactured by the Zirconium Corporation of America) closed at one end (Fig. 1). The brass head also housed a glass tube with a Pt lead sealed in it, and a gas inlet tube. The ZrO_2–CaO (nominally 7·5 wt% CaO) tube was inserted in the furnace, and the closed end, which was platinized over a length of 4·5 cm, was in the even temperature zone of the furnace. The Pt coating was deposited from a solution of chloroplatinic acid in ethyl alcohol, which was reduced by oils of rosemary and lavender; the reduction was carried out at 200–300°C, the product appearing to be a continuous shiny layer of the metal. Platinum wire was twisted around this platinized layer and connected to the sealed Pt lead in the brass head of the reaction tube assembly to serve as one electrode connection. The other electrode of the cell was formed inside the ZrO_2–CaO tube from a 2 mm diameter Pt ball with a Pt lead connection, which was pressed to the inner wall of the tube by means of a

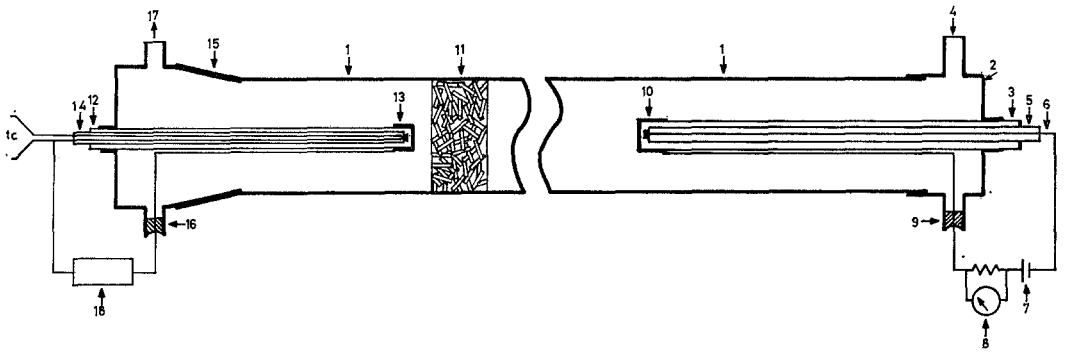

Fig. 1. Schematic diagram of the apparatus with 1: alumina reaction tube; 2: brass head supporting the electrolysing tube, the electrode connections and the gas inlet; 3: calcia stabilized zirconia tube, 12·7 mm o.d.; 4: gas inlet; 5: spring-loaded alumina rod; 6: Pt electrode serving as anode (air) in the electrolysing circuit; 7: d.c. potential source; 8: known resistance with millivoltmeter in parallel arrangement; 9: sealed Pt connection joining the Pt cathode; 10: platinized section of the stabilized zirconia tube and Pt cathode connection; 11: gas-mixer silica tube fragments; 12: calcia stablized zirconia tube, 6·35 mm o.d. used as oxygen meter; 13: platinized section with Pt lead; 14: Pt–13%Pt/Rh thermocouple and supporting tube spring-loaded against the inner end of the zirconia tube; 15: Pyrex cone and socket; 16: sealed Pt-electrode connection; 17: gas outlet; 18: digital voltmeter.

spring-loaded alumina rod. The atmosphere of the inner electrode was air.

A Pyrex cone was attached to the other end of the alumina reaction tube by means of epoxy resin. The socket which was joined to the cone carried a 6·3 mm diameter calcia stabilized zirconia tube, closed at one end, which was used to measure the oxygen content of the gas, a sealed-in Pt lead for electrode connection to this tube, and a gas outlet tube to a glass bubbler. One end of this ZrO_2–CaO tube which also carried a Pt–Pt/Rh thermocouple, spring-loaded against the inner end of the ZrO_2–CaO tube, was open to the air. One wire of the thermocouple was used as the electronic lead for the reference electrode. The outer surface of the closed end of this measuring tube was platinized and connected by means of a Pt lead to the sealed Pt connection in the Pyrex socket. The smaller ZrO_2–CaO tube was immersed in the furnace atmosphere downstream from the electrolysing tube, at a point where the temperature was approximately 100°C lower than that in the centre of the furnace, the two tubes being separated by approximately 20 cm. A gas mixer, made of small silica tubes, was placed between the two ZrO_2–CaO tubes to ensure the uniformity of the composition of the gas which passed over the measuring system. The ZrO_2–CaO tube which was used for measuring the oxygen potential was flushed with air, before each reading was taken, in order to eliminate errors due to polarization and thermal segregation.

The electromotive force of the oxygen meter was measured continuously by means of a Solatron Digital Volt Meter which has an input impedance of $5 \times 10^8 \Omega$. The thermocouple potential was measured by means of a Cambridge potentiometer, Type 44228. The electrolysing potential was obtained from a stabilized d.c. source Type SB 20/10, manufactured by Farnell Instruments Ltd., Yorks, England. The electrolysing current was determined from the potential drop across a known resistance, which was incorporated in the circuit.

2.2. *Gases*

The principal gas used throughout these experiments was 'O_2 free', nitrogen, supplied by the Canadian Oxygen Co., which has a nominal impurity content of 5 ppm H_2O (Dew point: −59°C). The oxygen content of this gas was increased, when required, by the controlled addition of compressed air through a long, very fine glass capillary.

The CO_2 content of the gas was adjusted, where required, by admixing, through a flowmeter, known volumes of nitrogen containing

0·18% (1800 ppm) CO_2, supplied by Matheson Co. of Canada.

In some experiments, dry nitrogen was required: the cylinder nitrogen stream was then passed through drying towers containing $CaCl_2$, $Mg(ClO_4)_2$ and P_2O_5, in that order.

For the experiments in which H_2O additions were made, the water partial pressure of the gas was fixed by bubbling through a fritted glass tube into an aqueous solution of sulphuric acid of the requisite concentration. After each experiment, the final density of the sulphuric acid was determined.

From a knowledge of the density and the ambient temperature, the water content of the gas passing through the solution could also be determined from tabulated data [6, 7]. The reliability of this procedure has been checked in a previous study [8].

Throughout this work, a total flow-rate of gas through the alumina reaction tube was maintained constant at 150 ml/min. This value of mass flow was selected as a matter of experimental convenience.

2.3. *Procedure*

The furnace temperature was adjusted to the required level and the initial oxygen chemical potential of the gas mixture was measured by means of the oxygen potential meter. The temperature of the meter was also observed since the initial oxygen partial pressure in the gas phase was calculated using the well-known relationship:

$$E = \frac{RT}{nF} \ln \frac{P_{O_2,\,air}}{P_{O_2,\,initial}} \qquad (1)$$

where E is the voltage measured by the oxygen meter;

R, F, are the gas constant and Faraday's constant respectively;

T is the temperature of the oxygen meter, °K;

P_{O_2} is the oxygen partial pressure.

The electrolysing d.c. voltage was then applied to the main zirconia tube, the air electrode having positive polarity (anode). The applied voltage was noted, together with the steady-state current, and the emf of the gas composition resulting from the electrolysis. After each electrolysing step, the voltage was switched off and gas was passed until the initial gas composition was regained. The voltage range scanned was $0{\cdot}5 < E_{appl.} < 3{\cdot}0$ V.

Electrolysis was applied to gases of different compositions at 800, 900 and 1000°C.

3. Results and Discussion

3.1. *The Efficiency of electrolysis*

In the preliminary experiments. it was found that the nitrogen supply, after drying, had an oxygen partial pressure of $10^{-4{\cdot}48}$ atmospheres and applying 1·40 V would reduce the oxygen partial presssure to $10^{-5{\cdot}20}$ at 1000°C. If the flow rate was increased above the standard value of 140 ml/min, the final P_{O_2} in the gas after electrolysis, was higher. This is to be expected if the quantity of oxygen which was removed remained constant. If, however, the gas was not dried prior to electrolysis, the oxygen potential of the gas was lowered to a much greater extent, corresponding to an oxygen partial pressure of $10^{-16{\cdot}0}$ atmospheres. The indication was that free oxygen cannot therefore be removed completely by electrolysis from the gas, but if water is also present, it too will be electrolysed and the resulting hydrogen will react with the remaining oxygen and thus lower the oxygen potential. A range of gas compositions was then subjected to electrolysis, the oxygen content being varied between 17 and 226 ppm, and the water content between dried gas, having approximately 0·01 ppm H_2O to 450 ppm H_2O.

Experiments were also conducted in which the water vapour was replaced with equal quantities of carbon dioxide. These experiments yielded the same results for corresponding partial pressures of CO_2 and H_2O, supporting the assumption that the product of the electrolysis of the oxygen-bearing gas, CO_2 or H_2, recombines with the remaining oxygen. Figs. 2–4 show the relative change in oxygen content as a function of the applied electrolysing voltage, and also how this depends on the composition of the gas mixture at temperatures 800, 900 and 1000°C. The relative decrease of O_2 content is defined as

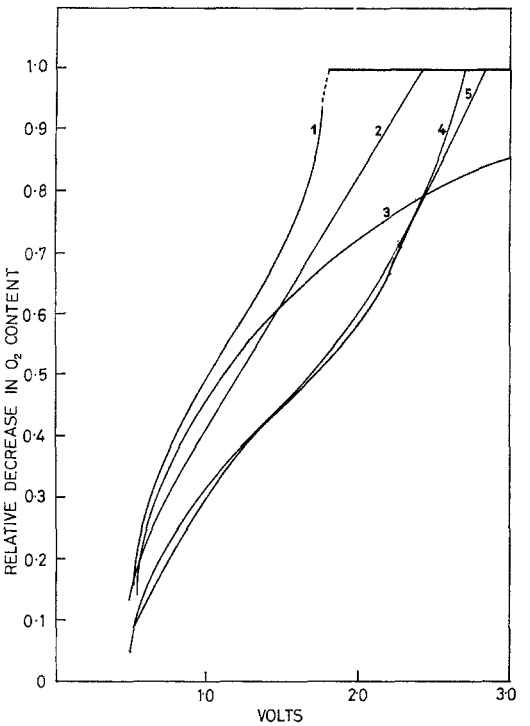

Fig. 2. Relative decrease of oxygen content of the gas, plotted against the electrolysing potential. Temperature 800°C; flowrate 140 ml/min.
1: 18 ppm O_2, 460 ppm H_2O; 2: 18 ppm O_2, 50 ppm H_2O; 3: 18 ppm O_2, dried gas; 4: 37 ppm O_2, 460 ppm CO_2; 5: 24 ppm O_2, 50 ppm CO_2.

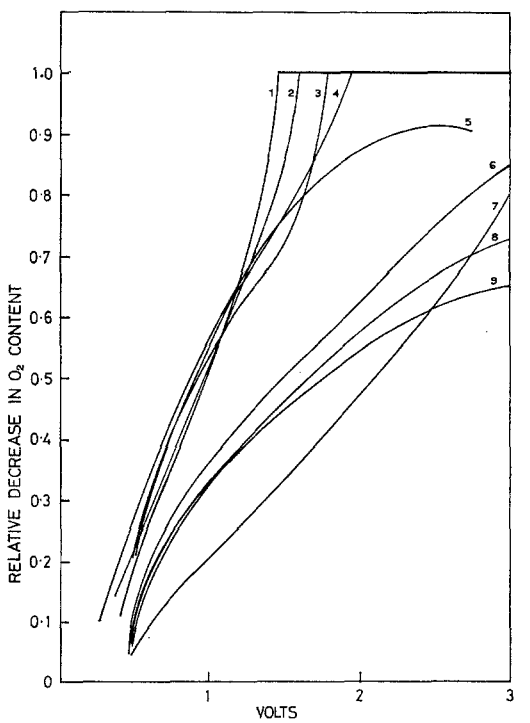

Fig. 3. Relative decrease of oxygen content of the gas, plotted against the electrolysing voltage. Temperature 900°C; Flowrate 140 ml/min. 1: 21 ppm O_2, 460 ppm H_2O; 2: 21 ppm O_2, 50 ppm H_2O; 3: 36 ppm O_2, 460 ppm CO_2; 4: 33 ppm O_2, 50 ppm CO_2; 5: 21 ppm O_2, dried gas; 6: 112 ppm O_2, 50 ppm CO_2; 7: 84 ppm O_2, 460 ppm H_2O; 8: 84 ppm O_2, 50 ppm H_2O; 9: 84 ppm O_2, dried gas.

$$\frac{\text{decrease in } O_2 \text{ ppm due to electrolysis}}{\text{initial } O_2 \text{ ppm in the gas}} \quad (2)$$

The value of this ratio was arbitrarily taken as unity when the oxygen partial pressure was reduced by more than eight powers of ten, which is tantamount to the virtual elimination of oxygen. At this stage, the amount of water electrolysed, and thus the volume of hydrogen produced, was equal to twice the volume of oxygen left in the gas after electrolysis.

It can be seen from these curves that the smaller the initial oxygen content of the gas, the lower the P_{H_2O} at which complete removal of free oxygen can be effected. As would be expected from the value of the free energy of formation of water, at lower temperatures a higher P_{H_2O} was required to produce sufficient amounts of hydrogen after electrolysis to react with the remaining oxygen.

The addition of CO_2 to dried N_2 gas had a similar effect to that of equal amounts of water. A completely quantitative analysis is not possible since the addition of CO_2 was accompanied by a slight increase of the oxygen content due to the finite oxygen content of the CO_2 source. Practically complete removal of oxygen then occurred at somewhat higher applied potentials. This is also expected because of the difference in the free energies of formation of H_2O and CO_2 respectively at the same temperature.

It can be concluded that at a constant temperature, the higher the initial oxygen content, the higher the amount of oxygen-bearing gaseous compound that is required to reduce the P_{O_2} to a very low level. Furthermore, at constant temperature, for the same initial oxygen content in the gas mixture, the higher the partial pressure of the oxygen-bearing gas component, the lower the value of the applied

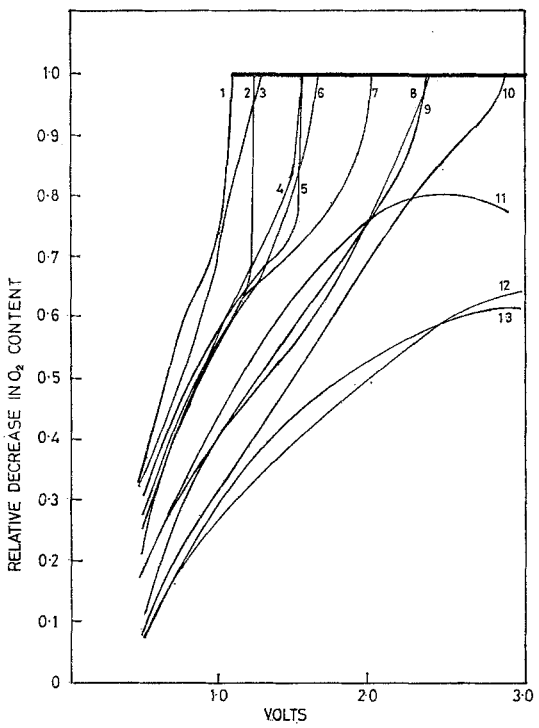

Fig. 4. Relative decrease of oxygen content of the gas plotted against the electrolysing voltage. Temperature 1000°C; Flowrate 140 ml/min. 1: 33 ppm O_2, 460 ppm H_2O; 2: 33 ppm O_2, 50 ppm H_2O; 3: 46 ppm O_2, 460 ppm CO_2; 4: 82±8 ppm O_2, 460 ppm H_2O; 5: 33±2 ppm O_2, dried gas; 6: 93 ppm O_2, 460 ppm CO_2; 7: 106 ppm O_2, 50 ppm CO_2; 8: 225 ppm O_2, 460 ppm CO_2; 9: 82±8 ppm O_2, 50 ppm H_2O; 10; 226±16 ppm O_2, 460 ppm H_2O; 11: 82±8 ppm O_2, dried gas; 12: 226±16 ppm O_2, 50 ppm H_2O; 13: 226±16 ppm O_2, dried gas.

potential at which complete removal of oxygen can be affected.

Comparing the results obtained at different temperatures, the electrolytic efficiency is further lowered as the temperature is decreased, due to the adverse effect of the increased electrical resistance of the solid electrolyte.

The experimental results in Figs. 2–4 show the expected effect that the rate of removal of oxygen from the gas phase is proportional to the applied electrolysing voltage. Where the 'complete reduction' of the oxygen potential is not achieved by electrolysis, the efficiency of the electrolysis appears to level off as the applied voltage approaches the decomposition voltage of ZrO_2. This effect is probably the result of the electrochemical reduction of the electrolyte tube when some of the oxygen ions constituting the current through the tube are not replaced from the gas. Thus, the net effect is a decrease in the electrolytic efficiency in the gas phase. The decomposition voltage calculated from the free energy of formation for ZrO_2, is $E^{\circ}_{ZrO_2}$ = 2·19, 2·24 and 2·28 V, at 1000, 900 and 800°C respectively.

The above experiments also serve to illustrate that gaseous electrolysis of oxygen-bearing compounds like H_2O, CO_2, SO_2 will only be effective if the initial free oxygen content of the gas is considerably lower than that of the gas to be removed. Furthermore, the reduced product of the electrolysis will react with the oxygen still available in the gas phase, reforming the electrolysed gas. The applied potential at which electrolysis of the oxygen-containing gas will take place depends on its standard free energy of formation, the partial pressure and the temperature.

3.2. *Relationship between the applied voltage and the electrolysing current*

The electrolysing currents are plotted against the applied voltage in Figs. 5–7, at temperatures 800, 900 and 1000°C respectively, for nitrogen gas containing different amounts of oxygen, water and carbon dioxide. It is clearly shown that the magnitude of the current depends primarily on the initially-present free oxygen in the gas. These current-voltage curves appear to have three easily-definable regions:

(1) Relatively linear, comprising the regions up to

$$E_{\text{Appl.}} \leqslant 1{\cdot}70 \text{ V at } 800^{\circ}\text{C}$$
$$E_{\text{Appl.}} \leqslant 1{\cdot}60 \text{ V at } 900^{\circ}\text{C}$$
$$E_{\text{Appl.}} \leqslant 1{\cdot}40 \text{ V at } 1000^{\circ}\text{C}$$

(2) Middle region where current increases parabolically with the applied voltage, i.e., the total resistance appears to diminish with increasing voltage.

(3) In this region the current, having shown a minimum value, keeps rising, while the applied voltage is kept constant.

In the following, these three regions and their physical meanings will be discussed.

3.2.1. *Near-linear regions of current–voltage*

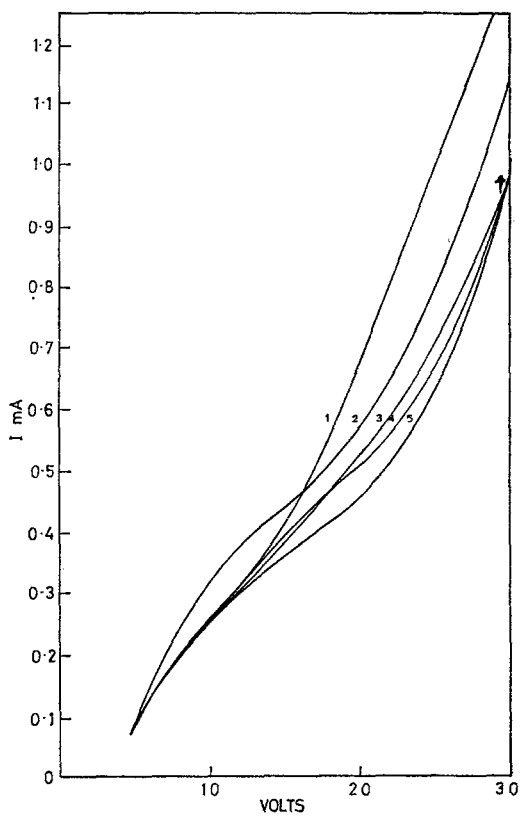

Fig. 5. Electrolysing voltage plotted against the current measured. Temperature 800°C. 1: 17 ppm O_2, 460 ppm H_2O; 2: 37 ppm O_2, 460 ppm CO_2; 3: 17 ppm O_2, 50 ppm H_2O; 4: 24 ppm O_2, 50 ppm CO_2; 5: 17 ppm O_2, dried gas. ↑ Current increased without increase in applied voltage.

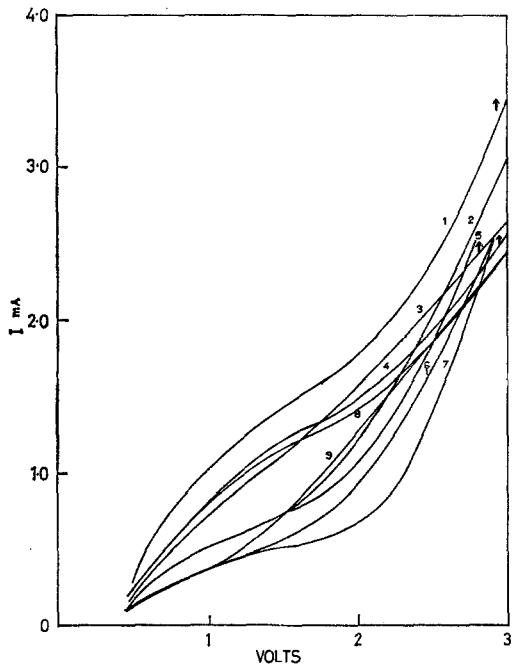

Fig. 6. Electrolysing voltage plotted against the current measured. Temperature 900°C. 1: 112 ppm O_2, 50 ppm CO_2; 2: 36 ppm O_2, 460 ppm CO_2; 3: 84 ppm O_2, 460 ppm H_2O; 4: 84 ppm O_2, 50 ppm H_2O; 5: 33 ppm O_2, 50 ppm CO_2; 6: 21 ppm O_2, 50 ppm H_2O; 7: 21 ppm O_2, dried gas; 8: 84 ppm O_2, dried gas; 9: 21 ppm O_2, 460 ppm H_2O. ↑ Current increased without increase in applied voltage.

curves. The electrolysing current in this section was found to be independent of time, a steady value being attained as soon as the electrolysis commenced. The gas returned to its initial composition immediately after the voltage had been switched off, allowing for the few seconds required for the gas to reach the oxygen meter in the furnace.

The slope of the tangent to each curve is a measure of the total resistance of the electrolysing circuit. It may be deduced that the reaction

$$1/2\,O_{2(\text{furnace atmosphere})} + 2e \rightarrow O^{--}{}_{(\text{Pt cathode})} \quad (i)$$

contributes considerably to the total resistance, since it was observed that the slope of the curves depends more strongly on the initial oxygen content of the gas mixture than if this process were at equilibrium. This step would be at equilibrium if some subsequent step such as (*ii*) or (*iii*) were rate-determining. If any of the processes

$$O^{--}{}_{(\text{cathode})} \longrightarrow O^{--}{}_{(ZrO_2)} \quad (ii)$$

$$O^{--}{}_{(ZrO_2)} \longrightarrow O^{--}{}_{(\text{Pt anode})} \quad (iii)$$

$$O^{--}{}_{(\text{Pt anode})} \longrightarrow 1/2\,O_2 + 2e \quad (iv)$$

were the main contributors to the circuit resistance, the slope would be independent of the available oxygen present in the gas phase.

The current values increase most rapidly with increased voltage at the lower applied voltages ($E_{\text{Appl.}} < 0{\cdot}7$ V). Thus the current–voltage relationship is initially non-linear. A similar effect was observed by Kroger *et al.* [5b] who attributed the effect to the fact that boundary layer diffusion was the rate-controlling step at low applied voltages and in the region of oxygen partial pressures employed in the present study.

The electrical potential difference can be

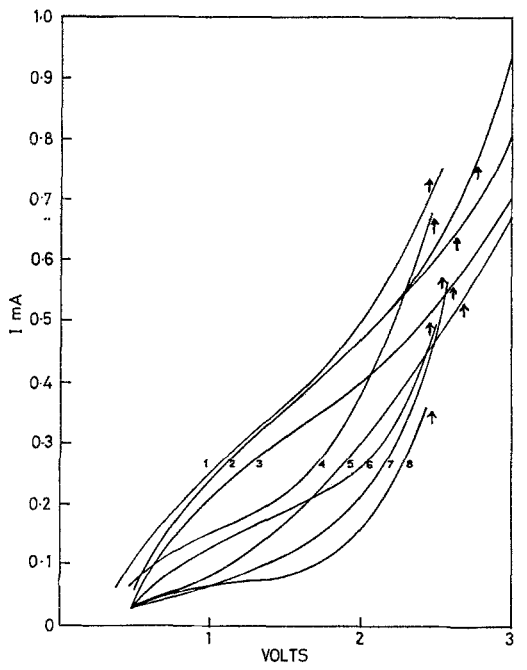

Fig. 7 Electrolysing voltage plotted against the current measured. Temperature 1000°C. 1: 225 ppm O_2, 460 ppm CO_2; 2: 226±16 ppm O_2, 460 ppm H_2O; 226±16 ppm O_2, dried gas; 3: 226±16 ppm O_2, 50 ppm H_2O; 4: 93 ppm O_2, 460 ppm CO_2; 5: 33±2 ppm O_2, 460 ppm H_2O; 6: 82±8 ppm O_2, 50 ppm H_2O; 82±8 ppm O_2, dried gas; 7: 33±2 ppm O_2, 50 ppm H_2O; 8: 33±2 ppm O_2, dried gas. ↑ Current increased without increase in applied voltage.

represented by the following schematic distribution:

$$E_{\text{Appl.}} = E_{\text{cell}} + I\,[R_1 + 2R_2 + R_3 + R_4] \quad (3)$$

where E_{cell} is the emf of the galvanic cell set up by the difference in the oxygen partial pressures, $P_{O_2(\text{air})}$ and $P_{O_2(\text{furnace})}$. The expression also comprises the sum of the IR drops, which represents the potential gradient necessary to attract the oxygen molecules out of the flowing gas system on to the cathode and discharge them into air, in the opposite direction to that in which the thermodynamic activity gradient would tend to drive them. These symbols have the following interpretations:

R_3 represents the electrolyte resistance; thus IR_3 is the potential difference required to move the oxygen ions through the electrolyte.

R_4 results from the electrode reaction, and the discharge of oxygen in air:

$$2O^{--}{}_{(\text{Pt anode})} \longrightarrow O_{2(\text{air})} + 4e$$

R_2 is related to oxygen ions entering or leaving the zirconia phase from the Pt electrode.

Finally, IR_1 is the potential required to drive the oxygen molecules across the boundary layer and to ionize them in the Pt electrode:

$$4e + O_{2(\text{furnace gas atmosphere})} \longrightarrow 2O^{--}{}_{(\text{Pt cathode})}$$

Thus, the circuit can be schematically represented as:

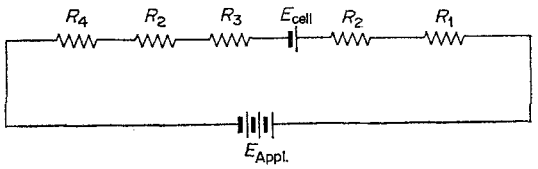

R_4, which is the resistance due to discharge under constant conditions throughout the experiments, and R_3 which is the ionic resistivity of the electrolyte, may be considered constant at a constant temperature.

The processes which give rise to resistances R_2 and R_1 occur in series at the cathode, and any apparent variation in the total resistance of the electrolysing circuit when the oxygen level is changed should then be due to these. The concentration of oxygen in the Pt foil must depend under equilibrium conditions on the square root of the oxygen pressure in the gas phase, and this was not found to be the case. It is impossible to say whether the oxygen in solution in platinum is ionized or not, since the oxygen pressure dependence of the adsorption would be the same. This is because the free electron concentration in the equilibrium constant

$$1/2\,O_2 + 2e \rightarrow O^{--} \qquad K = \frac{C_{O^{--}}}{P_{O_2}^{\frac{1}{2}} \cdot C_e^2}$$

remains sensibly constant.

Under the given experimental conditions, the resistance due to individual steps in the electrolytic process could not be separately measured. Only the ohmic resistance of the solid electrolyte and the total resistance of the circuit could be obtained from these measurements.

The calculated total resistance of the electrolysing circuit over this region at 1000°C was found to be:

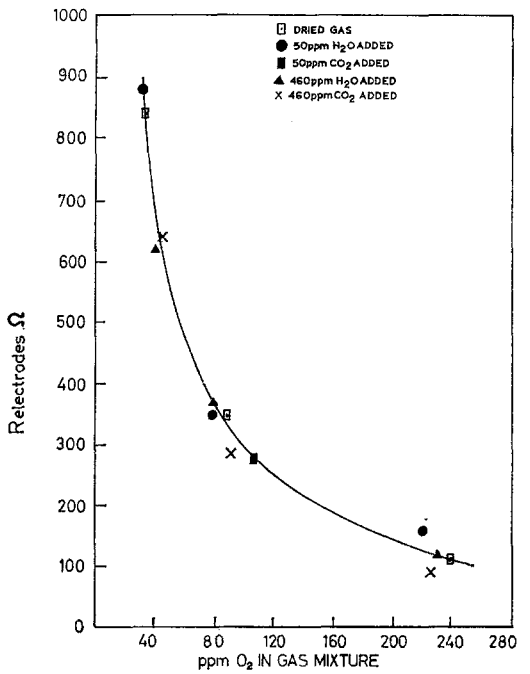

Fig. 8. The calculated resistance of the electrodes during electrolysis, shown as a function of the oxygen content of the gas. Temperature 1000°C; electrolysing voltage 1 V.

$R_T = 1{\cdot}43 \times 10^3$ Ω when the O_2 content is 32 ± 2 ppm,
$R_T = 0{\cdot}65 \times 10^3$ Ω when the O_2 content is 82 ± 8 ppm, and
$R_T = 0{\cdot}36 \times 10^3$ Ω when the O_2 content is 226 ± 16 ppm.

Since $E_{\text{Appl.}}$, I and $R_{\text{electrolyte}}$ (referred to as R_3 in the general expression (3)) are known, it is possible to calculate

$$R_{\text{electrodes}} = \frac{E_{\text{Appl.}}}{I} + \frac{RT}{nFI} \ln \frac{P_{O_2 f}}{P_{O_2 \text{air}}} - R_{\text{electrolytes}} \quad (4)$$

On Fig. 8, $R_{\text{electrodes}}$ is plotted against the free oxygen content of the gas mixtures, at 1000°C, at a constant applied voltage of 1·00 V. It can be seen that the electrode resistance decreases as the free oxygen content of the gas is increased, in a manner which is independent of the water vapour or carbon dioxide content.

Table 1 shows that the product of the P_{O_2} and $R_{\text{electrodes}}$ appears to be constant at constant temperature and applied voltage, indicating that the resistance under consideration is a linear function of the oxygen partial pressure. This suggests that the electrode process is diffusion-controlled. However, classical boundary layer calculations using $D(O_2 \text{ in } N_2) = 0{\cdot}174$ at 0°C and 1 atmosphere [12], adjusted to the tempera-

Table 1.

(Temperature = 1000°C $E_{\text{Appl.}} = 1{\cdot}0$ V)

$R_{\text{electrodes}}$ calculated as in Equation (4) Ω	Initial P_{O_2} of gas $\times 10^{+6}$	Other oxygen-bearing gases present in gas $\times 10^{+6}$	$P_{O_2} \times R_{\text{electrodes}}$ $\times 10^{+3}$
154	220	50 (H_2O)	33·88
348	80	50 (H_2O)	27·84
880	32	50 (H_2O)	28·16
118	230	460 (H_2O)	27·14
110	238	—	26·18
620	40	460 (H_2O)	24·80
840	33	—	27·72
366	79	—	28·91
345	84	460 (H_2O)	28·98
274	106	50 (CO_2)	29·07
285	91	460 (CO_2)	25·91
90	225	460 (CO_2)	20·25
638	45	460 (CO_2)	28·69
		Mean value:	27·50 ± 3·07

tures employed in these experiments, give boundary layer thicknesses of the order of 1–2 cm, which are clearly too high under these conditions. The activation energy of the electrode processes was found to be 6·6 kcal. which is also higher than would be expected from diffusion control. Molecular adsorption requires activation energies of this magnitude. Thus, adsorption may be the slowest step in the process occurring at the electrode. Clearly, further research is required to elucidate the nature of the electrode reactions.

3.2.2. *Non-linear regions of current–voltage curves.* At applied voltages higher than 1·70, 1·60 and 1·40 V at temperatures 800, 900 and 1000°C respectively, the electrolysing current has higher values than anticipated from a linear ohmic relationship; in effect the total resistance of the circuit appears to have diminished. The ionic transport number for ZrO_2–CaO was shown to be near unity at 1000°C in the oxygen pressure range $1–10^{-15}$ atmospheres, by several authors [9, 10, 11]. Thus, as long as both $P_{O_2(air)}$ and $P_{O_2(cathode)}$ fall within this region there should be no electronic contribution to the conductivity of the solid electrolyte and a linear potential drop can be assumed across the thickness of the electrolyte. In this case

$$R_{tube} = \frac{K_{ionic} \times l}{A} \Omega$$

where K_{ionic} = the specific ionic resistance of the solid electrolyte at the temperature
A = area of the platinized surface of the electrolyte
l = wall thickness of the electrolyte tube.

The voltage required to move the oxygen ions across the electrolyte, as part of the total applied potential, is

$$E' = IR_{tube}$$

Above a certain applied voltage, depending on the temperature, $P_{O_2 cathode}$ in the term E_{cell} (c.f. Equation (1)) will fall in the oxygen potential range where ZrO_2–CaO no longer shows electrolytic behaviour and t_{ion} is no longer close to unity. In this case

$$E' = E^i + E^{ni}$$

where E^i is the potential range in which only electrolytic conduction takes place and E^{ni} is where $t_{ion} \neq 1$. A schematic representation of the potential distribution in these situations can be seen in Figure 9(a) and (b).

The section of the electrolyte tube wall where the external potential drop falls below that of the electrolytic region will be depleted of oxygen ions, leaving vacancies in the lattice and uncompensated positive charges. These latter are subsequently compensated by electron injection from the cathode. As the electrolysing voltage is switched on, and until an internal steady state is achieved in the electrolyte, the flux of oxygen

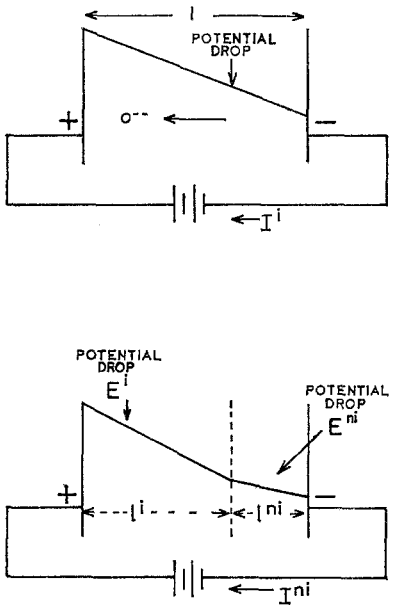

Fig. 9. Schematic representation of ionic transport across the electrolyte.
(a) Only ionic conduction present.
$I^i \propto n\, O^{--}{}_{(gas)} = 2\, n\, e$
Current in electrolyte = current in external circuit = number of oxygen ions entering at cathode. l = thickness of electrolyte.
(b) Section of electrolyte is non-ionic conductor.
$E' = E^i + E^{ni}$
$l = l^i + l^{ni}$ = total thickness of electrolyte
(i) Initial current $= I_i^{ni} \propto n'\, O^{--}{}_{(gas)} + m\, O^{--}{}_{(electrolyte)}$
= total ionic current in ionic section, I^i
Also $I_i^{ni} \propto n'\, O^{--} + 2\, m\, e = 2\,(n' + m)\, e$
Initial current in external circuit = total current in non-ionic section, I^{ni}
(ii) Steady current $= I^{ni} \propto n'\, O^{--}{}_{(gas)} = 2\, n' e$
Current in electrolyte = current in external circuit.
$I^i < I^{ni} < I_i^{ni}$

ions providing the current, will only partly be obtained from the gas atmosphere near the cathode. The balance will originate in the semi-conducting section created in the solid electrolyte.

The electronic conductivity of the unchanged solid electrolyte section will still be close to zero. Since this section is in series with the semi-conducting section, the electronic contribution to the *total* conductivity of the solid electrolyte will still be approximately zero. In time, a steady state is achieved and the flux of oxygen ions across the solid electrolyte is only composed of oxygen ions derived from molecules in the gas phase, the same number of oxygen molecules leaving at the anode as entered at the cathode. The value of the current will be higher in the steady state than expected from the application of Ohm's Law to the original wall thickness, because the effective thickness of the electrolyte wall has been diminished. Thus

$$R'_{\text{tube}} = \frac{K_{\text{ionic}} \times l^{\text{i}}}{A} + \frac{K^{\text{ni}} \times l^{\text{ni}}}{A} < R_{\text{tube (as meausured initially)}}$$

The specific ionic resistivity in the semi-conducting section is here denoted by K^{ni}, and this probably has a lower value than K_{ionic}, since the oxygen ion mobility would be higher in this section following the creation of a large number of randomly distributed vacancies on the lattice. In making this conclusion, it is assumed that the decrease in conductivity with increasing vacancy concentration which is observed in well-annealed samples of ZrO_2–CaO is the result of ordering of the vacancies at higher concentrations.

The above considerations are supported by the observation that, as the electrolysing voltage was increased, the initial values of the current were higher, before gradually dropping to the steady values, which are represented as I on Figs. 5–7. The time required to reach steady values of current increased as the magnitude of the applied voltage increased. Conversely, when the voltage was switched off, it required an increasing length of time (5–30 min) with increasing voltage, for the gas composition to return to the initial, non-electrolysed oxygen partial pressures. These observations indicate that solid state diffusion is the rate-determining step and also that as $E_{\text{Appl.}}$ is increased, I^{ni} as represented in Fig. 9(b), also increases at the expense of I^{i}. Furthermore, the lower the temperature of the electrolysis, the higher the applied voltage at which the solid state reaction became noticeable, as is to be expected from the stability-temperature dependence of zirconia.

3.23. *Region of increasing current.* In regions of applied voltage where

$$E_{\text{Appl.}} \geqslant -\frac{\Delta G_T^\circ}{nF}$$

ΔG_T° being the free energy of formation of zirconia from oxygen-saturated zirconium and oxygen; the electrolysis current first drops in value, before it increases continuously. The rate of increase in the current beyond the minimum was faster with increasing temperature. At these potentials, the electrolytic/semi-conducting boundary in the electrolyte moves across the total thickness of the wall of the tube, providing both oxygen ions and injected electrons as carriers. As the electrolysis progresses, the number of charge carriers increases continuously. The experiment was not allowed to reach a steady state, in order to avoid causing permanent damage in the solid electrolyte tube.

It should be noted that the voltage at which noticeable electrolysis of the solid electrolyte began was slightly higher for gas compositions richer in oxygen. This suggests that the oxygen ions removed from the solid by reduction were partially replaced from the gas phase, thus maintaining a thin electrolytic layer on the anode side at higher voltages than was the case with lower oxygen contents.

4. Acknowledgement

The authors wish to thank the National Research Council of Canada for supporting this investigation.

References

[1] H. H. Mobius, *Z. Phys. Chem.* (Leipzig), **223** (1966) 425.
[2] C. M. Diaz and F. D. Richardson, *Trans. Inst. Min. Metall.*, **76** (1967) 196.
[3] R. Sridhar and J. H. E. Jeffes, *Ibid.*, **76** (1967) C-44.

[4] L. Heyne in 'Mass Transport in Oxides', U.S. Dept. of Comm. National Bureau of Standards Spec. Publication 296, p. 149.
[5] D. Yuan and F. A. Kroger, *J. Electrochem. Soc.*, **116** (1969) 594; H. Yanagida, R. J. Brook and F. A. Froger, *Ibid*, **117** (1970) 593.
[6] 'Handbook of Chemistry and Physics', The Chemical Rubber Co., Cleveland, Ohio, (1969–70) 50th ed., p. F-7.
[7] 'Chemical Engineering Handbook' (Ed. J. H. Perry), 4th ed. p. 168, McGraw-Hill, New York (1963).
[8] C. B. Alcock, S. Zador, and B. C. H. Steele, *Proc. Brit. Ceram. Soc.*, No. 8 (1967) 231.
[9] H. Schmalzried, *Z. Elecrochem.* **66** (1962) 572.
[10] B. C. H. Steele and C. B. Alcock, *Trans. Met. Soc. AIME*, **233** (1965) 1369.
[11] R. A. Rapp. in 'Symposium on Thermodynamics of Nuclear Materials', I.A.E.A. Vienna, Sept. 1967.
[12] S. Dushman, 'Vacuum Technique', John Wiley, New York (1949).